

Supplementary Information

for

Suppressed Spectral Blue-shift in ZnS-coated CuInS₂ Quantum Dots for Efficient Luminescent Solar Concentrators

Changhong Cheng ^{1, †}, Jiayi Zhang ^{2, †}, Yufan Wu ², Jingjian Zhou ³, Qiliang Fu ⁴, Ilya
Sychugov ³, Dan Shan ¹, Bo Xu ^{2, *} and Jing Huang ^{1, *}

¹ School of Environmental and Biological Engineering, Nanjing University of Science and Technology, Nanjing 210094, China. Email: jinghuang@njust.edu.cn

² Key Laboratory for Soft Chemistry and Functional Materials of Ministry of Education, School of Chemistry and Chemical Engineering, Nanjing University of Science and Technology, Nanjing 210094, China. Email: boxu@njust.edu.cn

³ Department of Applied Physics, KTH Royal Institute of Technology, Stockholm 11419, Sweden.

⁴ Co-Innovation Center of Efficient Processing and Utilization of Forest Resources, College of Materials Science and Engineering, Nanjing Forestry University, Nanjing 210037, P.R. China.

Section 1. Experimental details

S1.1 Chemicals

Zinc acetate ($\text{Zn}(\text{Ac})_2$, 99.99%), Zinc oleate ($\text{Zn}(\text{OA})_2$, Purum), Zinc iodide (ZnI_2 , Purum), Zinc Chloride (ZnCl_2 , Purum), copper(I)iodide (CuI , 99.99%), indium acetate ($\text{In}(\text{Ac})_3$, 99.99%), sulfur powder (S, 99.99%), 1-dodecanethiol (DDT, 99.9%), oleic acid (OA, 97%), oleylamine (OAm, 97%), octadecene (ODE, 90%), trioctylphosphine (TOP, 97%), Pentaerythritol Tetra(3-mercaptopropionate) (thiol monomers), pentaerythritol tetrakis (3-mercaptopbutylate) (PE1), triallyl-1,3,5-triazine-2,4,6(1H,3H,5H)-trione (alkene monomers), 1-hydroxycyclohexyl phenyl ketone (Irgacure-184,99%), toluene.

S1.2 Synthesis of CuInS_2 core QDs

To synthesize CIS core QDs, 0.5 mmol of CuI , 0.5 mmol of $\text{In}(\text{Ac})_3$, and 5 ml of DDT were placed in a round bottom three-necked flask, with a magnetic stir in the Schlenk line system under N_2 atmosphere. The mixture was then heated to 120 °C until the solid powder was completely dissolved. The temperature was then increased to 235 °C and the reaction was carried out for 20 min to obtain the required QDs. Finally, the mixture was cooled to room temperature for subsequent use.

S1.3 Synthesis of CIS/ ZnS -DDT QDs

8 mL of ODE, 4 mmol of $\text{Zn}(\text{Ac})_2$ and 8 mmol of DDT were placed in a round bottom three-necked flask. The mixture was evacuated and heated to 120°C under N_2 to prepare Zn-DDT. After the solution was clarified, the prepared CIS core was injected into the solution. The temperature was then quickly raised to 240 °C and kept for 1h to prepare Zn shell-1 solution. In another 100 mL round-bottom flask, a zinc oleate solution was prepared by mixing 8 mL of ODE, 4 mmol of $\text{Zn}(\text{Ac})_2$ and 8 mmol of OA were mixed. The mixture was heated to 120 °C under N_2 protection to prepare Zn-OA solution. After complete dissolution, the Zn-OA solution was slowly injected into the reaction solution of the QDs with thin ZnS shell-1 (1 ml/min), and kept for 1 h to form CIS/ ZnS QDs with gradient alloy shells. Then, the reaction was allowed to

cool naturally. The QDs were purified by repeated precipitation and re-dispersion with ethanol and toluene. Finally, the QDs were dispersed in toluene.

S1.4 Synthesis of CuInS₂/ZnS-Zn(OA)₂

In the overcoating procedure, 2 mL of original CIS core solution was diluted with 3 mL of 1-octadecene (ODE) and then degassed three times. For growth of a ZnS shell, a mixture of 0.4 mmol of zinc oleate, 0.4 mmol of sulfur dissolved in trioctylphosphine (1 M solution), and 4 mL of ODE was added dropwise into the reaction solution at 200 °C and kept for 20 min before the flask was cooled down. The QDs were purified by repeated precipitation and re-dispersion with ethanol and toluene. Finally, the QDs were dispersed in toluene.

S1.5 Synthesis of CuInS₂/ZnS-ZnI₂

For the synthesis of CuInS₂/ZnS-ZnI₂ QDs, the zinc iodide was used as zinc precursor, and other procedures were the same as in the preparation of CuInS₂/ZnS-Zn(OA)₂ QDs.

S1.6 Ligand exchange with zinc thiolate ligand

In a vial, 5 mmol of ZnCl₂, 1 mL of OAm, 15 mmol of PE1 were mixed at room temperature. Then the mixture was stirred for approximately 6 hours, gradually transforming into a yellow transparent solution (denoted as Zn-PE1 solution). Subsequently, 10 ml of toluene solution containing CIS/ZnS QDs (15 mM) was added to 5 ml of the Zn-PE1 solution. After stirring for 30 min, 30 ml of ethyl acetate were added, and the mixture was centrifuged. The solid precipitate was identified as CIS/ZnS-Zn-PE1 QDs.

S1.7 Fabrication of LSC devices

Disperse the QDs solid in 13 g of trimethylolpropane triacrylate (alkene monomers) to obtain a clear and transparent mixture. Then, 37 g of tetrakis(3-mercaptopropionate) pentaerythritol ester (thiol monomers) and 0.4 g of Irgacure-184 (initiators) was added to the solution. Subsequently, the mixture was mixed thoroughly by ultrasonication for 10 minutes, followed by placing the mixture in a vacuum desiccator to remove bubbles in the solution. Slowly pour the mixture

solution into a prepared glass mold, and cure it with 360 nm ultraviolet light for 30 seconds to initiate the thiol-ene polymerization reaction. To obtain a uniform nanocomposite interlayer, the UV light intensity should be kept below $0.1 \text{ mW}\cdot\text{cm}^{-2}$. The polymerization is completed after storing the sample in the dark for 1 hour.

S1.8 Characterizations and measurements

Transmission Electron Microscopy (TEM) measurements were performed on an TECNAI G2 20 LaB6 microscope (Schottky emitter), and operated at an accelerating voltage of 200 kV. Powder X-Ray Diffraction (XRD) patterns were acquired in Bragg–Brentano geometry with Cu K α radiation (Bruker-AXS D8 Advance powder diffractometer).

Optical Measurements: The PL spectra of the QDs were obtained using a spectrometer (Cary Eclipse, Agilent, Austria). The UV–vis light absorption spectra were obtained by Shimadzu UV-3150 UV–vis–NIR spectrometer. Time-resolved PL was determined using a Hamamatsu C11367 Quantaurs-Tau system with an excitation wavelength of 405 nm. The absolute PLQY was measured using a Horiba Fluorolog system equipped with a single grating and a Quanta-Phil integration sphere coupled to the Fluorolog system. FTIR measurements were performed using JASCO-FT/IR-4700, and the FTIR spectra of the QDs were recorded in the attenuated total reflectance (ATR) mode (4 cm^{-1}). Transmittance and haze measurements of the LSC were conducted by following our previous work, with a set-up consisted of light source, integrating sphere and signal acquisition system.

Photovoltaic Measurements: The photovoltaic performance of the LSCs was investigated using a large-area LED-based solar simulator (Sunbrick from G2V optics, 350–1100nm spectral range, ASTM E927 class AAA+, $25 \times 25 \text{ cm}^2$) and carried out by applying an external potential bias (from 0 to 6V) to the device while recording the generated photocurrent with a Keithley model 2450 digital source meter. One edge of the LSC device was attached with a solar cell (IXYS, IXOLARTM, SM141K08L, $88 \times 15 \text{ mm}$), with excess parts on the solar cells were

covered by black tape. The rest edges were also covered by black tape. To block direct illumination to the solar cell, a roof with width of 5 mm was applied on top of the solar cell. For I - V measurements using the back reflector, a piece of white paper was placed under the LSCs at a distance of 6 cm.

the PCE value can be calculated by the following equation.

$$PCE_{LSC} = \frac{I_{SC} \cdot V_{OC} \cdot FF \cdot 4}{I_0 \cdot A_{top}} \quad S1$$

where I_{SC} , V_{OC} , FF were obtained directly from the measured I - V curves, I_0 is the light intensity of AM1.5 G, which is 0.1 W/cm², and A_{top} is the surface area of the LSCs, and its value was 77.44 cm² (8.8×8.8 cm²).

Section 2. Calculation of waveguiding efficiency

η_{wvgd} is a waveguiding efficiency, which is one of the most important parameters in LSC. For a square shape LSC with a side length l , it can be evaluated as

$$\eta_{wvgd} = \frac{M_1(2\alpha lk/\sqrt{\pi}) \cdot \alpha \cdot \sqrt{\pi}}{\delta(\alpha_{sc} + QY \cdot \alpha_{re}) \left(lk\alpha + M_1\left(\frac{2\alpha lk}{\sqrt{\pi}}\right) \cdot \sqrt{\pi} \right) - lk\alpha^2} \quad S1$$

where α [cm^{-1}] is the sum of scattering α_{sc} [cm^{-1}], reabsorption α_{re} [cm^{-1}], and matrix absorption α_{mx} [cm^{-1}] coefficients: $\alpha = \alpha_{sc} + \alpha_{re} + \alpha_{mx}$; δ is a waveguiding fraction ($\sim 75\%$ for $n = 1.5$, which is unity minus escape cone losses of 25%). k is a coefficient for 3D geometry: $k \approx 1.14$ for $n = 1.5$; $M_1(\xi)$ is a modified Struve function of the second kind.

Section 3. Structural characterization of CIS/ZnS QDs

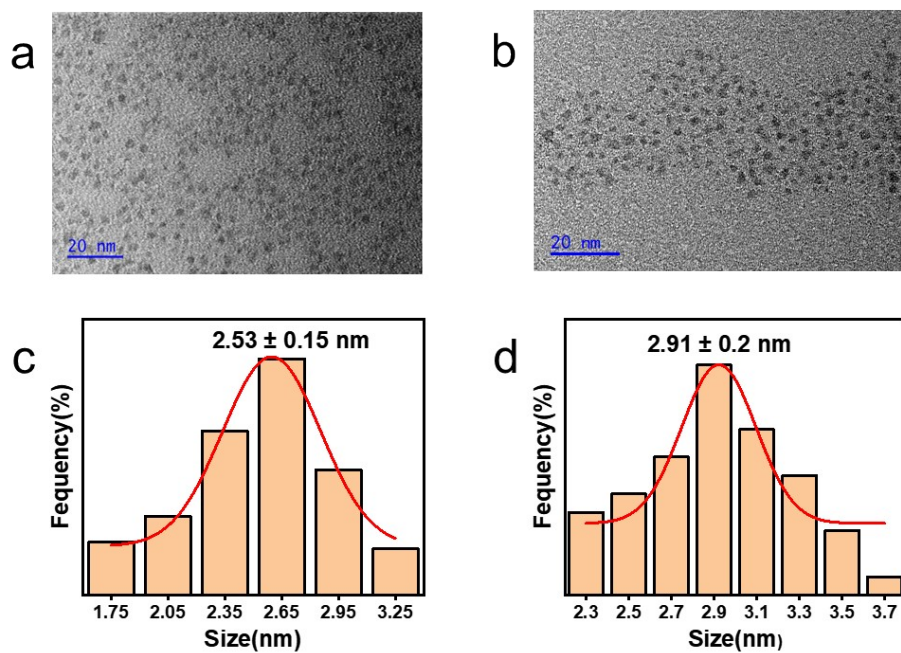


Figure S1. TEM images and particle size distribution of CIS QDs (a,c) and CIS/ZnS-Zn(OA)₂ QDs (b,d).

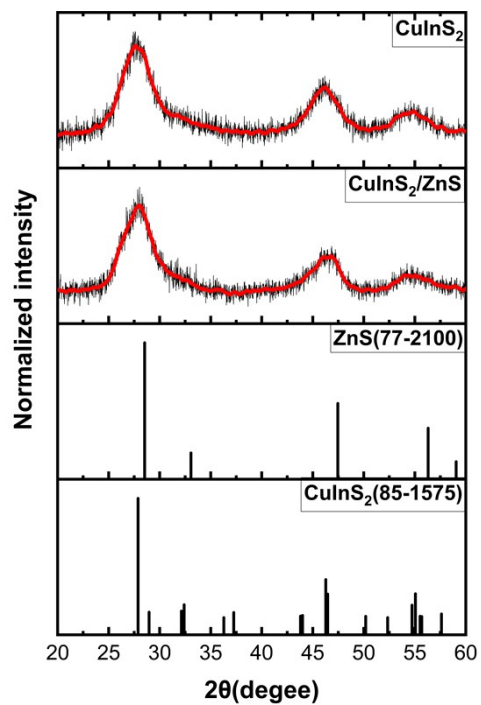


Figure S2. XRD of the as-synthesized CIS QDs and CIS/ZnS-Zn(OA)₂ QDs.

Table S1. Lattice parameters of CIS core and CIS/ZnS core/shell QDs determined based on the XRD patterns

| Material | Peakposition(degree) | Assigned Peak (hkl) | d-spacing (Å) | a (Å) |
|----------|-----------------------|---------------------|---------------|-------|
| CIS | 27.87 | (111) | 3.20 | 5.54 |
| | 46.85 | (202) | 1.94 | 5.48 |
| | 55.25 | (311) | 1.66 | 5.51 |
| CIS/ZnS | 28.20 | (111) | 3.16 | 5.47 |
| | 46.90 | (202) | 1.93 | 5.46 |
| | 55.60 | (311) | 1.65 | 5.47 |

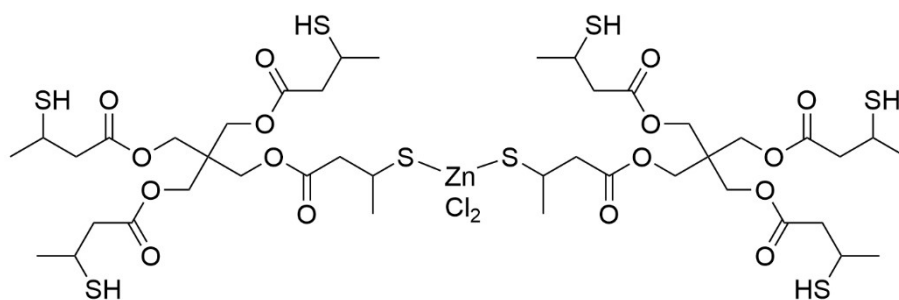


Figure S3. Molecular structure of Zn-PE1.

Section 4. calculation of AVT, optical efficiency and waveguiding efficiency of the LSC device

AVT was calculated as the integral of the transmission spectrum and AM 1.5G photon flux weighted against the photopic response of the human eye:

$$AVT = \frac{\int T(\lambda) \cdot V(\lambda) \cdot AM1.5G(\lambda) d\lambda}{\int V(\lambda) \cdot AM1.5G(\lambda) d\lambda} \quad S2$$

where $T(\lambda)$ is the transmission spectrum of the LSC and $V(\lambda)$ is the human eye photopic response.

The optical efficiency refers to the ratio of the number of photons emitted from the edge of a photovoltaic device to the number of photons incident upon it. it could be calculated as :

$$optical\ efficiency = \frac{p_{out}}{p_{in}} = \frac{J_{edge}}{J_{Si} \times G} \quad S3$$

where J_{edge} is the current density when solar cells are installed at the edge of the device and J_{Si} the current density of solar cells illuminated by solar simulator directly. G is geometric factor of the LSC device, which is defined by the ratio of the top area (A_{top}) and the edge area (A_{edge}).

Waveguiding efficiency of the LSC was derived by following the equation, with measured PLQY of QDs in OSTE, PCE under black ground, and calculated solar absorption ratio:

$$PCE = \frac{eV_{oc}}{h\nu_{abs}} \cdot FF \cdot EQE_{cell} \cdot A_{QD} \cdot QY \cdot \delta \cdot \eta_{wvgd}$$

S4

Section 5. Performance of LSC based on CIS/ZnS-DDT-PE1 QDs

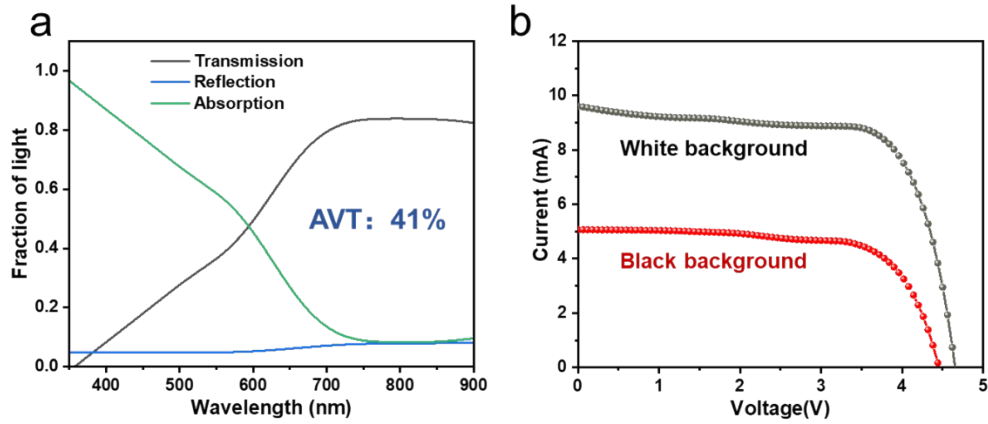


Figure S4. Aesthetic quality (a) and I - V curves (b) measured for of the fabricated LSC based on CIS/ZnS- Zn(OA)₂-PE1 QDs, with black background and white background.

Table S2. Comprehensive comparison of state-of-the-art fluorophores for LSCs

| Fluorophores | Waveguide | Dimensions (cm ²) | η_{opt} (%) | PCE (%) | Ref |
|--|-------------------------------------|-------------------------------|------------------|--------------------------------------|-----------|
| CIS/ZnS | off-stoichiometric thiol-ene (OSTE) | 9×9×0.3 | 9.69 | 1.17 ^a /2.23 ^b | This work |
| CIS/ZnS | PLMA | 10×10 | 8.1 | 2.94 | 1 |
| CIS/ZnS | OSTE | 9×9 | / | 2.09 ^a /3.56 ^b | 2 |
| ZCISe/ZnSe | PMMA | 10×10×0.5 | 3.59 ± 0.12 | 0.44 | 3 |
| CZISe/ZnSe | poly(lauryl methacrylate) (PLMA) | 2×2×0.2 | 3.67(liquid) | 0.83(liquid) | 4 |
| CuInS ₂ /ZnSe _x S _{1-x} | polyvinylpyrrolidone (PVP) | 10×10×1.0 | 0.53 | / | 5 |
| CuInS ₂ /ZnS | PMMA | 2.2×2.2×0.3 | 26.5 | 8.71 | 6 |

| | | | | | |
|--|--|--------------|--------------|--------------------------------------|----|
| Cu _{2-x} Se@SiO ₂ @ CuInSe _{2-x} S _x /ZnS | PLMA | 6×6×0.3 | 1.38 | 0.23 | 7 |
| CuInSe _{2-x} S _x | toluene | 9.5×9.5×0.77 | 11.7(liquid) | | 8 |
| CuGaInS ₂ /ZnS | toluene | 5×5×0.5 | 6.54 | 0.48 | 9 |
| CuInSe _{2-x} S _x /ZnS | polydimethylsiloxane (PDMS) | 5×5×0.9 | / | 1.19 | 10 |
| | | 5×5×0.3 | / | 0.50 | |
| carbon dots@ CuInSe _{2-x} S _x /ZnS | poly(lauryl methacrylate) and ethylene glycol dimethacrylate (PLMA-co-EGDM) | 10×10×0.5 | / | 0.46 | 11 |
| | | 5×5×0.5 | / | 0.58 | |
| | | 3×3×0.5 | / | 0.62 | |
| | | 2×2×0.5 | / | 0.67 | |
| D-π-A Organic Dyes(TP-6CF3) | PMMA | 20×5×0.6 | 5 | 0.25 | 12 |
| Silicon QDs | PLMA | 12×12×0.26 | 2.85 | / | 13 |
| Silicon QDs | OSTE | 20×20×0.3 | / | 0.77 ^a /1.57 ^b | 14 |
| Pb-Perovskite QDs | 1,2-ethanedithiol (EDT) | 10×10×0.001 | 3 | 2.87 | 15 |

^a mesasured against a black background; ^b mesasured against a white background.

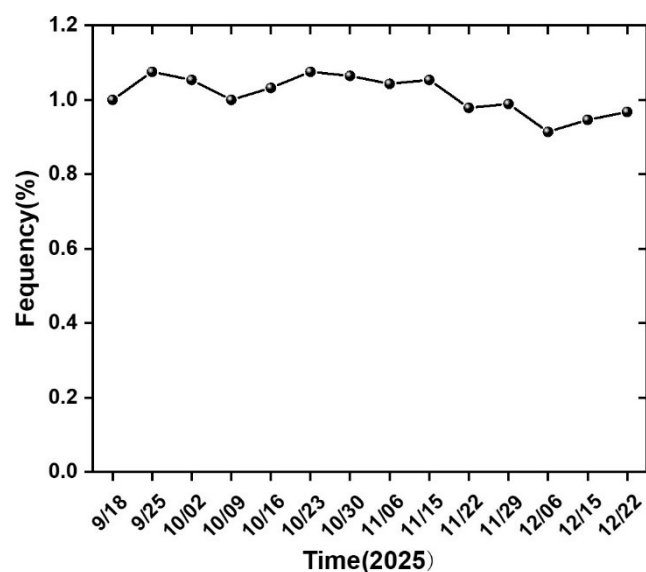


Figure S5. Change in PCE values for LSC based on CIS/ZnS-Zn(OA)₂-PE1 QDs during outdoor stability test.

Reference

1. M. R. Bergren, N. S. Makarov, K. Ramasamy, A. Jackson, R. Guglielmetti and H. McDaniel, *ACS Energy Lett.*, 2018, **3**, 520–525.
2. Y. F. Wu, J. Huang, J. Y. Zang, J. J. Zhou, C. H. Cheng, Z. Hu, D. Shan, W. X. Yang, I. Sychugov, L. C. Sun and B. Xu, *Energ Environ. Sci.*, 2024, **17**, 6338–6349.
3. Y. Q. Chen, F. Y. Ge, Y. L. Lai, L. J. Wang, X. L. Zhao, R. L. Wang, S. Peng, X. J. Wu and Y. F. Zhou, *ACS Appl. Mater. Interfaces*, 2024, **16**, 14072.
4. X. Liu, B. Luo, J. Liu, D. Jing, D. Benetti and F. Rosei, *J. Mater. Chem. A*, 2020, **8**, 1787–1798.
5. D. C. J. Neo, W. P. Goh, H. H. Lau, J. Shanmugam and Y. F. Chen, *ACS Appl. Nano Mater.*, 2020, **3**, 6489–6496.
6. C. Li, W. Chen, D. Wu, D. Quan, Z. Zhou, J. Hao, J. Qin, Y. Li, Z. He and K. Wang, *Sci. Rep.*, 2015, **5**.
7. Y. Lai, Y. Chen, L. Wang, X. Zhao, K. Zheng, J. Zhong, X. Tong, R. Wang, F. Rosei and Y. Zhou, *Nano Energy*, 2025, **135**, 110632.
8. K. Gungor, J. Du and V. I. Klimov, *ACS Energy Lett.*, 2022, **7**, 1741–1749.
9. H. Zhi, X. Tong, Y. You, A. I. Channa, X. Li, J. Wu, G. S. Selopal and Z. M. Wang, *Sol. RRL.*, 2023, **7**.
10. Y. Chen, F. Ge, Y. Lai, L. Wang, X. Zhao, R. Wang, S. Peng, X.-J. Wu and Y. Zhou, *ACS Appl. Mater. Interfaces*, 2024, **16**, 14072–14081.
11. L. Wang, Y. Chen, Y. Lai, X. Zhao, K. Zheng, R. Wang and Y. Zhou, *Nanoscale*, 2024,

- 16**, 188–194.
12. E. Tatsi, V. Raglione, G. R. Ragno, S. Turri, G. Mattioli, F. Porcelli, D. Caschera, C. Botta, G. Zanotti and G. Griffini, *J. Mater. Chem. C*, 2025, **13**, 14465–14477.
 13. F. Meinardi, S. Ehrenberg, L. Dharmo, F. Carulli, M. Mauri, F. Bruni, R. Simonutti, U. Kortshagen and S. Brovelli, *Nat. Photonics*, 2017, **11**, 177–185.
 14. J. Huang, J. Zhou, E. Jungstedt, A. Samanta, J. Linnros, L. A. Berglund and I. Sychugov, *ACS Photonics*, 2022, **9**, 2499–2509.
 15. B. Mendewala, E. T. Vickers, K. Nikolaidou, A. DiBenedetto, W. G. Delmas, J. Z. Zhang and S. Ghosh, *Adv. Opt. Mater.*, 2021, **9**, 2100754.